International Journal for Housing Science and Its Applications
Publish August 10, 2025. Volume 46, Issue 4 Pages 2128-2143

https://doi.org/10.70517/ijhsa464182

Numerical simulation study on the impact of steel temperature control technology in refining furnaces on energy consumption

Wen Qiu[1,*], Zhenlong Zhao[2], Jian Huang[1], Zhangman Liu[1], Hongyan Luo[1] and Baolong Li[1]
[1] Benxi Beiying Iron and Steel (Group) Co., LTD. Steel Plant, Benxi, Liaoning, 117017, China
[2] Nanjing Dongchuang Xintong Internet of Things Research Institute Co., LTD., Nanjing, Jiangsu, 210000, China
Corresponding authors: (e-mail: 13941421170@163.com).

Abstract With the continuous progress of science and technology and the intensification of the pace of national industrialization, the demand for energy is also increasing, and the introduction of temperature control technology can realize the reasonable control of energy under the premise of meeting the needs of production or construction. This paper analyzes the smelting process of LF refining furnace and establishes the temperature forecasting model and alloy charging model. Then the differential variational operator and immune cloning operator are introduced on the basis of artificial bee colony to propose an improved artificial bee colony algorithm, and artificial neural network is used to establish an intelligent model for steel temperature forecasting, followed by simulation experiments. The experimental results show that the steel temperature forecasting model in this paper has higher forecasting accuracy and stronger generalization ability than the traditional mechanism model and neural network model for steel temperature forecasting. Pareto's law is applied to determine the main factors affecting energy consumption, and the main factor is smelting power in the electric furnace process. The model was put into use with an average power saving of about 10.8kW-h per ton of steel, which reduced the production cost.

Index Terms artificial neural network, LF refining furnace, artificial neural network, energy consumption, temperature prediction modeling

I. Introduction

A refining furnace is an important piece of equipment in the metallurgical field, used for high-temperature refining and impurity removal of metal alloys to improve product purity and mechanical properties [1], [2]. Its working principle is primarily based on the differences in melting points and volatility of metal alloys [3]. In a refining furnace, metal alloys are heated to melt them, and then the molten metal containing impurities is heated and held at a constant temperature. Impurity elements gradually evaporate or oxidize based on their different volatilities, thereby achieving the refining objective [4]-[6]. The refining furnace process generally includes steps such as preheating, melting, refining, and cooling, each of which requires strict temperature control [7], [8]. For the refining furnace steelmaking process, temperature is critical. It is not only the foundation of the steelmaking process but also the basis for achieving good ingot quality [9], [10].

The level of temperature control in the refining furnace directly affects key indicators such as steel consumption, alloy consumption, and refractory material consumption, thereby determining the cost of steelmaking [11], [12]. Effective and balanced system temperature control at low temperatures is crucial for ensuring smooth production, improving product quality, and reducing production costs [13], [14]. In refining furnace temperature control, the most critical step is controlling and regulating molten steel temperature, which directly impacts the quality of continuous cast ingots and energy consumption [15]-[17]. Energy consumption in the steelmaking process primarily includes heating of raw materials, reduction reactions, oxidation reactions, and steel cooling [18], [19]. Among these, high-temperature smelting is one of the most energy-intensive stages in steel production [20]. However, the steel temperature control process also requires significant energy input. To ensure steel quality, cooling is typically applied using steel temperature control technology, a process that consumes large amounts of water and electricity [21]-[23].

Reference [24] developed a hybrid model combining metallurgical mechanisms, Isolation Forest (IF), Zero-Component Analysis Whitening (ZCA Whitening), and Deep Neural Networks (DNN), aimed at predicting molten steel temperature during the ladle refining process in a Ladle Furnace (LF), providing a reference for achieving precise control of molten steel temperature during LF refining. Reference [25] proposed a method for predicting the endpoint temperature of LF steelmaking by combining case-based reasoning (CBR) and Bayesian belief networks

(BBN), aiming to improve the control level of the endpoint temperature of LF steelmaking. Based on case analysis, it was found that CBR-BBN has better prediction accuracy for the endpoint temperature of molten steel in LF refining. Literature [26] points out that LF refining can effectively control the temperature of molten steel, and by using models for control and decision-making during LF refining, refining operations can be further standardized, thereby improving the quality and stability of molten steel. Literature [27] points out that in the prediction of LF final molten steel temperature, some nonlinear influencing factors can affect the prediction accuracy. To address this issue, an improved case-based heat transfer calculation reasoning model was established, and experiments demonstrated the effectiveness of this model. Literature [28] reviews modeling methods for temperature prediction, slag formation, and other models based on the primary tasks of the LF refining process, describes the advantages and disadvantages of each modeling method, and proposes a future technical framework based on existing work, aiming to advance the modeling and intelligent development of the LF refining process. Literature [29] proposes an instance-based reasoning method for predicting the end temperature of LF, aiming to improve the temperature control level of LF. It also proposes a two-step retrieval method based on CBR and a feature-weighted method based on relevance to accurately predict the temperature, revealing that the CBR method can effectively predict the end temperature of LF molten steel. Literature [30] emphasizes that high-precision prediction of the final temperature of converter steel is a crucial foundation for achieving intelligent metallurgy in the converter process, and proposes a modeling method based on the Bayesian formula, verifying that this method further improves prediction accuracy. Literature [31] highlights the importance of accurately predicting the final temperature of molten steel for controlling LF refining and proposes an error correction method based on case-based reasoning (CBR), EC-CBR, aimed at reducing prediction model errors. The effectiveness of this method for data-driven models and mechanism models is validated. Literature [32] introduces the important role of accurately predicting molten steel temperature and proposes a dynamic ensemble regression model for predicting molten steel temperature, aiming to improve the accuracy of existing data-driven prediction models. The superiority of the aforementioned method is proven through experiments. Literature [33] proposes a tree-structured ensemble generalized regression neural network (TSE-GRNNs) method to accurately control molten steel temperature within the LF. Based on this method, a temperature model is constructed, revealing that it achieves higher accuracy than existing temperature models and meets the error requirements for LF molten steel temperature prediction. Literature [34] emphasizes the importance of temperature control during LF refining and introduces a non-contact steel temperature monitoring system, demonstrating that the system can measure LF furnace steel temperature without affecting the smelting process, offering more convenient and safer operation. Reference [35] proposes an interval-type radial basis function neural network system for predicting molten steel temperature during secondary metallurgical monitoring and control, revealing that this approach effectively reduces the frequency of instrument replacement under high-temperature damage conditions. The above studies emphasize the importance of molten steel temperature control during the refining furnace process, primarily in terms of ensuring system safety, improving molten steel quality, and enhancing stability, and propose temperature measurement and prediction methods based on deep neural networks and instance reasoning.

The study firstly introduces the overall structure and process flow of LF furnace and clarifies the importance of temperature and composition control in the smelting process. Aiming at the shortcomings of the artificial bee colony algorithm, differential variational operator and clonal expansion operator are introduced, and the improved artificial bee colony algorithm (GABC-ELM) is proposed to establish an intelligent model for steel temperature forecasting by using artificial neural network, and the core algorithm of the intelligent model adopts the optimized Extreme Learning Machine of the improved artificial bee colony algorithm. The neural network was trained using the particle swarm algorithm, the parameters in the model were set, and the temperature forecasting model was simulated using Matlab. The main factors affecting energy consumption in the production process were identified using the Pareto principle, and sensitivity calculations of variable parameters were performed using sensitivity factor analysis.

II. LF refining process and modeling

II. A.LF refining process

II. A. 1) LF furnace

The overall structure of LF refining furnace mainly consists of charging system, electrode system, argon blowing system, feeding system, temperature measurement and sampling system, ladle furnace body and furnace cover, the main systems will be introduced in the following. the schematic diagram of LF equipment is shown in Figure 1.

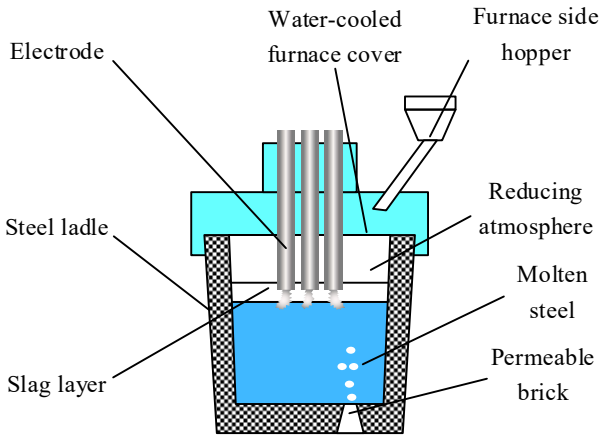

Figure 1: Schematic diagram of ladle furnace body

II. A. 2) LF Furnace Process Flow

The general process flow of LF furnace refining is as follows:

(1) LF furnace steel generally from the electric arc furnace, from the electric arc furnace out of the steel before the lf furnace need to be connected to argon, check whether the argon pipeline is smooth. Before leaving the steel, the operator will carry out temperature measurement and sampling, and transfer the temperature and composition information into the system as the initial composition of the LF furnace reference.

(2) The molten steel is transported from the electric arc furnace to the LF heating station, during which the operator will observe the slag condition and molten steel quantity for reference.

(3) After the molten steel arrives at the processing station, the furnace cover is lowered first, and then according to the steel type and the molten steel condition, aluminum particles, pre-molten slag and white ash are added, and the electrode under the electrode starts to be heated, and the heating method is submerged arc heating - that is to say, the graphite electrodes are buried inside the material layer, and the heating time and the gear position are decided mainly according to the steel type and the temperature of steel, and the slag stage is not consumed at one time, and it needs to be added several times. The white ash and pre-molten slag cannot be consumed at one time and need to be added several times. The main purpose of slag is to remove oxygen, sulfur and inclusions in steel, while the slag covering the surface of the liquid steel can also prevent the liquid steel and air contact.

(4) After the end of the slag for the first time in the LF furnace sampling temperature measurement, during the observation of the slag condition, to determine whether the need to make up the white ash or pre-melting slag, after the completion of the sample delivery according to the target temperature and the rhythm of the production to control the heating gear and time.

(5) After receiving the sample back from the laboratory, calculate the amount of alloy to be added according to the composition content and target composition content, and judge whether it is necessary to add white ash according to the sulfur content.

(6) After the end of heating, take the second temperature measurement and sampling to judge whether the temperature and composition are qualified, and if not, make fine adjustments.

(7) According to the production rhythm to control the heating gear and time, 15-20 minutes before the steel to adjust the oxidizable metal composition, and then feed the line, feed the line after the soft blowing of argon, in the process of soft blowing temperature measurement and take the third sample, if the temperature and composition of the qualified and the rhythm of production allows, out of the station.

II. B.LF Furnace Temperature Forecasting Model

II. B. 1) Temperature control

Due to the complexity of the LF refining process, the models established only through the mechanism are usually less generalizable, less accurate, and there are a large number of unknown parameters, which often involve complex physicochemical processes, and a large number of experiments are needed to figure out the principles, and the development cycle is long and costly. The data forecasting model, through the collection of relevant data and then trained to get the temperature forecast results, data modeling only need to analyze the process variables affecting the temperature change of molten steel information, without the need to understand the complex physicochemical reaction mechanism, and modeling is simple, learning ability, so it can overcome the problems of the mechanism modeling. In this paper, by collecting data from 120tLF refining furnace of a steel plant, GRNN

network is used to establish a temperature forecasting model to realize continuous forecasting of molten steel temperature.

II. B. 2) Temperature forecasting model analysis

The analysis of the LF furnace liquid steel energy expenditure situation is mainly through the law of conservation of energy, through the analysis of the LF furnace refining process can be seen that the LF furnace liquid steel absorbed energy mainly from the arc heating and a small part of the alloy and liquid steel oxidation reaction exothermic. The energy into the ladle is mainly consumed through the following five parts: the first part is used for molten steel heating; the second part is the ladle through the energy lost by the lining; the third part is used to join the slag and alloy melting; the fourth part of the slag through the loss of heat, slag heat radiation and convection conduction will heat loss; the fifth part of the argon stirring loss of heat, the argon itself absorbs heat as well as the argon stirring leads to liquid steel bare. Argon stirring leads to liquid steel exposed will cause energy loss.

The energy balance expression of LF refining process is as follows:

$$Q_t = Q_{in} - Q_{chen} - Q_m - Q_f - Q_{Ar} \tag{1}$$

where, Q_t - Total energy change/J., Q_{in} - Electrical energy absorbed by the steel/J, Q_{chen} - Energy lost through the cladding/J, Q_m - Heat absorbed by charging /J, Q_f - Heat lost through the slag surface /J, Q_{Ar} - Heat loss due to argon blowing / J.

II. C.LF furnace alloy charging composition control model

Alloy composition content refers to the proportion of a certain alloying element in the steel, at this stage of the alloying element composition content of the calculation can be completed by the formula, alloying element content calculation formula is as follows:

$$a = \frac{Pb + Gc\eta}{P + G} \tag{2}$$

where, a - Elemental content in molten steel after addition of alloy, P - Weight of steel/kg, b - Content of the element in the steel before adding the alloy, c - Content of the component in the alloy, G - Amount of alloy added/kg, η - Alloy element yield.

According to the above formula, except for the elemental yield, the rest of the parameters can be directly determined by the system, only the elemental yield can not be accurately determined due to the influence of the physical and chemical properties of the elements, and with the change of smelting conditions and changes, so the accuracy of the elemental yield directly affects the accuracy of the alloy composition calculation. At the present stage, the judgment of alloy dosage by operators mainly relies on the fixed yield, so that the alloy composition cannot be adjusted to the target content by dosage at one time. Therefore, the accuracy of the alloy yield is not only related to the prediction of the current elemental composition, but also determines the amount of alloy added. The formula for calculating the alloy yield is as follows:

$$\eta = \frac{P(a-b)}{Gc} \tag{3}$$

where, η - Alloying element yield, P - Steel weight/kg, a --Target alloy element content, b --Element content in molten steel before alloy addition, G --Amount of alloy added/kg, c - Content of the component in the alloy.

The above formula can be used to calculate the actual yield of a certain smelting, the alloy yield used at this stage of production is the average value of the actual yield obtained through statistical calculation on the basis of a large number of smelting data.

The accuracy of the alloy element yield affects whether the alloy composition can be accurately and once completed fine-tuning will affect the production schedule. The fundamental factor affecting the alloying element yield is the chemical nature of the alloying elements, some elements with strong stability, such as copper, nickel, molybdenum, tungsten and other elements will not be oxidized due to the protection of iron, the element yield is relatively fixed; and aluminum, titanium, silicon, boron and other elements with overly active chemical properties are generally adjusted 10-20 minutes before the steel is discharged, and therefore not in the prediction model to consider the scope.

III. Intelligent model for steel temperature forecasting

III. A. Model preparation phase

III. A. 1) Data collection

Combined with the refining process and communication with field technicians, in the LF refining process affects the liquid steel temperature of the main factors are; ladle temperature on the line, the temperature of the liquid steel into the station, the temperature of the liquid steel out of the station, the smelting time, power consumption, argon consumption and the weight of the liquid steel, and these factors have different degrees of influence on the liquid steel temperature of the LF furnace end of the different steel grades, the current use of the production of a large number of steel grades of 42 CrMo4 as the object of the study. The study is now using the 42CrMo4 steel grade with larger production volume as the research object. Understanding that in 2022 the LF furnace in the refining process of the operating specifications and compared with previous years have been greatly improved, so the LF production data from January 1, 2022 to December 25, 2022 as a dataset, a total of 1573 groups were collected including the LF furnace incoming molten steel temperature, the total power consumption, the total argon consumption, the treatment cycle, white slag retention time, ladle temperature on the line, and the final molten steel weight, initial molten steel weight, and LF furnace terminal temperature, which are nine types of variables about 42CrMo4.

III. A. 2) Data pre-processing

In data mining, the massive amount of raw data exists a large number of incomplete, inconsistent, and abnormal data, which seriously affects the efficiency of the implementation of data mining modeling, and may even affect the bias of data mining, so in order to improve the quality of the data, it is necessary to deal with the abnormal values of the data, this paper adopts the method of 3σ for the abnormal values to be found and excluded, if the deviation of the sample data $X=\{x_1,x_2,\cdots,x_n\}$ is greater than 3σ, that is, it is considered to be this set of data is abnormal and it will be eliminated. Among them:

$$\sigma=\sqrt{\sum_{i=1}^{n}(x_i-\bar{x})^2/(n-1)} \tag{4}$$

The 1573 sets of 42CrMo4 dataset collected were culled for anomalous data using the rule of 3σ. After culling, the dataset remains

$$\rho_{X,Y}=\frac{\operatorname{cov}(X,Y)}{\sigma_X\sigma_Y}=\frac{E[(X-\mu_X)(Y-\mu_Y)]}{\sigma_X\sigma_Y} \tag{5}$$

The absolute value of Pearson's coefficient lies between 0 and 1. The larger its absolute value, the stronger the correlation between the two.

III. A. 3) Correlation analysis

Correlation analysis mainly determines the statistical association between two or more variables, and further analyzes the strength and direction of the association if it exists. In order to measure the correlation between variables, this paper utilizes the Pearson coefficient to evaluate the degree of correlation, and the formula is shown below:

$$\begin{aligned}\rho_{X,Y}&=\frac{\operatorname{cov}(X,Y)}{\sigma_X\sigma_Y}=\frac{E[(X-\mu x)(Y-\mu y)]}{\sigma_X\sigma_Y}\\&=\frac{\sum_{i=1}^{n}(X_i-\bar{X})(Y_i-\bar{Y})}{\sqrt{\sum_{i=1}^{n}(X_i-\bar{X})^2}\sqrt{\sum_{i=1}^{n}(Y_i-\bar{Y})^2}}\end{aligned} \tag{6}$$

III. B. Steel temperature prediction based on ELM and improved ABC algorithm

III. B. 1) Improved artificial bee colony algorithm

Artificial bee colony algorithm is by imitating the honey harvesting behavior of bees, after scholars to research and summarize the optimization method, its application process fully demonstrates the idea of cluster intelligence, the algorithm has an important feature is that he does not need to know more about it when solving the problem, and its principle of work is to compare the strengths and weaknesses of the problem faced by the established algorithms

to carry out a local search for the optimal The work is to compare the strengths and weaknesses of the problem, through the established algorithms for local optimization, and finally find the optimal solution that we need [36].

The convergence speed of the artificial bee colony is relatively slow and the problem of falling into local optimality occurs in the process of computation, in this paper we improve its performance by introducing differential variational operator and clonal expansion operator into the algorithm, and adopt the above two improvement methods to improve the performance of the artificial bee colony algorithm.

The improved artificial bee colony algorithm (GABC-ELM), for N training sample sets with different dimensions of D, is computed as follows:

(1) Hired bee search phase

The differential variation operator used inside the differential evolutionary algorithm is introduced into our algorithm in the search phase, and combined with the search process of the hired bees

$$v_{i,j} = x_{i,j} + rand[-1,1]\left(x_{best,j} - x_{k,j} + x_{l,j} - x_{m,j}\right) \tag{7}$$

where $x_{best,j}$ is the optimal individual of the current colony; $x_{k,j}$, $x_{l,j}$ and $x_{m,j}$ are three different individuals randomly selected in addition to the current individual, i.e. $i \neq k \neq l \neq m$.

(2) Follower bee following phase

In the updating process of following bees, we introduce the clonal amplification operator. In the calculation stage, the following bees are cloned according to the fitness of the following bees, and the number of clones is shown in the following equation:

$$N_i = \text{int}\left[SN \times fitness(x_i) \Big/ \sum^{SN} fitness(x_i) \right] \tag{8}$$

where N_i is the number of clones performed on the i nd follower bee and SN is the population size of the population; $fitness(x_i)$ is the value of the fitness calculated for the i th follower bee. When the following bee position information is changed, it will be selected by the resulting concentration position and fitness, and the food source with better fitness will be selected. The probability formula for concentration and the selection probability formula are as follows:

$$\begin{cases} P_d(x_i) = \dfrac{1}{SN}\left(1 - \dfrac{HN}{SN}\right) & \dfrac{N_i}{SN} > T \\ P_d(x_i) = \dfrac{1}{SN}\left(1 + \dfrac{HN}{SN} \times \dfrac{HN}{SN - HN}\right) & \dfrac{N_i}{SN} \le T \end{cases} \tag{9}$$

where N_i is the number of follower bees whose adaptation value is similar to the adaptation value of the i nd follower bee; N_i / SN is the proportion of follower bees with similar adaptation in the colony; T is the concentration threshold; and HN is the number of follower bees with a concentration greater than T. The selection probability is calculated as follows:

$$P_{choose}(x_i) = \alpha P_i(x_i) + (1-\alpha) P_d(x_i) \tag{10}$$

A roulette wheel is used for the selection of the newly generated group of following bees, and then it will be compared with the original food source on the basis of adaptation of memorization assessment, and if the adaptation becomes better, the new food source will be used to replace the previous food source.

(3) Scouting bee search phase

For a certain period of time if no update of the food source is generated, the role of the hired bee will be changed to a scout bee, and step (1) will be performed again and then the individual will be regenerated.

(4) The iteration ends when the fitness value reaches a certain precision or when the number of iterations reaches a set limit.

III. B. 2) Artificial Neural Networks

Artificial neural networks, referred to as neural networks or connectivity models, work as models that function in the distributed parallel processing of information by mimicking the behavioral properties of neural networks in animals, the complexity of the system is very important for such models, and the main in achieving the purpose of processing information is through the regulation of the relationship of the neural nodes within [37]. Artificial neural networks are applications similar to the structure of the mathematical model of synaptic coupling of the brain for information processing.

III. B. 3) Steel Temperature Prediction Models

In this paper, an improved artificial bee colony algorithm is used to optimize the implicit layer weights and thresholds of the Extreme Learning Machine (GABC-ELM), which can effectively improve the stability and accuracy of the Extreme Learning Machine, so that it can meet the actual requirements of industrial production sites.

(1) Initialization

Coding method:

$$\theta_G = \left[w_{1,G}^T, \cdots, w_{L,G}^T, b_{1,G}, \cdots, b_{L,G} \right] \tag{11}$$

According to the ELM algorithm, the encoding w_j is a D-dimensional vector, each dimension is a random number between -1 and 1, $j = 1, \cdots, L$; b_j is a random number between 0 and 1; and G is the number of iterations of the bee colony.

(2) Hired bee search phase

The differential variation operator used in the differential evolutionary algorithm is introduced into the algorithm in the search phase and combined with the search process of the hired bee:

$$v_{i,j} = x_{i,j} + rand[-1,1]\left(x_{best,j} - x_{k,j} + x_{l,j} - x_{m,j} \right) \tag{12}$$

where $x_{best,j}$ is the optimal individual in the current colony; $x_{k,j}$, $x_{l,j}$ and $x_{m,j}$ are randomly selected individuals but with the current individual removed, i.e. $i \neq k \neq l \neq m$.

(3) Follower bee following stage

In the updating process of following bees, we introduce the clonal amplification operator. In the calculation stage, the following bees are cloned according to the fitness of the following bees, and the number of clones is shown in the following equation:

$$N_i = \text{int}\left[SN \times fitness(x_i) \Big/ \sum^{SN} fitness(x_i) \right] \tag{13}$$

(4) Scout bee search phase

When there is no update to the food source for a certain period of time, the role of the hired bee will be converted to a scout bee, and step (1) is repeated to regenerate the individual.

(5) The iteration ends when the fitness value reaches a certain precision or the number of iterations reaches a set limit.

When the iteration ends, the connection weight w and threshold b of ELM are extracted from the optimal individual and verified.

GABC-ELM is used as the core algorithm of the intelligent model, and five main influencing factors are used as inputs to the intelligent algorithm, and the terminal temperature of molten steel is used as the output to establish an intelligent model for molten steel temperature prediction. The structure of the steel temperature prediction model for LF refining furnace based on GABC-ELM is shown in Fig. 2.

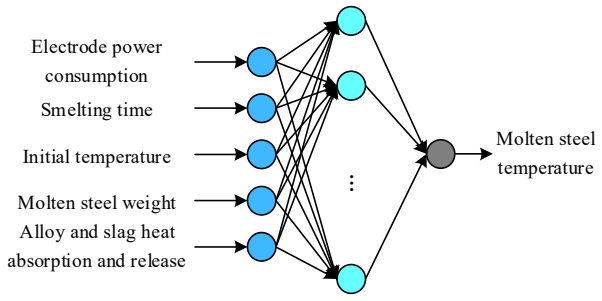

Figure 2: prediction model of molten steel temperathure based on GABC-ELM

III. C. Numerical simulation modeling

III. C. 1) Melt temperature prediction at finishing time

The samples for the temperature prediction model at the terminal moment are taken from the production data of 95 furnaces of RH refining furnaces of a steel plant from November to December 2022, in which 70% of them, totaling

61 groups, are taken as training samples, and the remaining 30%, totaling 22 groups, are taken as test samples.

The parameters of the particulate swarm algorithm were chosen as w_{max} =1.5, w_{min} =0.5, c_{max} =2.6, c_{min} =0.6.The number of neural network implicit layer units was chosen as 16, the number of iterations was chosen as 1000, and the target mean squared deviation was chosen as 5. The results are shown in Fig. 3, Fig. 4, Fig. 5 and Table 1. It was found that the training mean squared error was 15.06, the maximum error of prediction was -5.27, and the average mean squared error of prediction was 5.51. 95% accuracy was achieved within ±5°C of the forecast error, and 100% accuracy was achieved within ±6°C of the error.

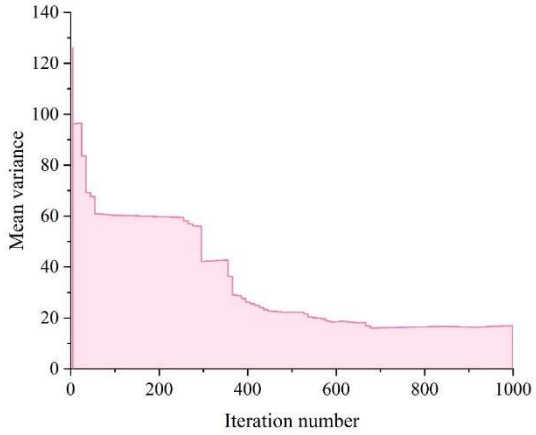

Figure 3: The RMS Training Error of end-point model

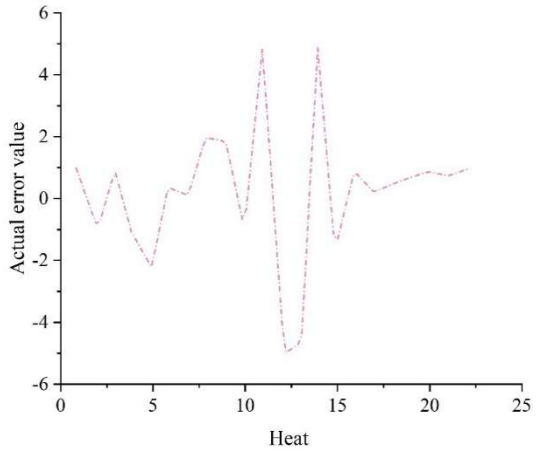

Figure 4: The prediction error of end-point model

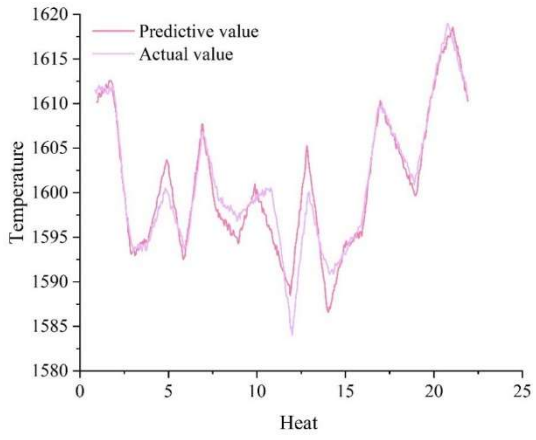

Figure 5: The temperature prediction effect of end-point model

Table 1: The temperature forecast data of end-point model

Heat	Forecast temperature (℃)	Error	Heat	Forecast temperature (℃)	Error
1	1621.47	0.87	12	1599.59	-5.25
2	1623.61	-1.27	13	1616.23	-4.89
3	1603.57	0.77	14	1596.64	4.7
4	1605.68	-1.34	15	1605.33	-1.99
5	1614.79	-2.45	16	1606.63	0.71
6	1603.13	0.21	17	1621.3	0.04
7	1618.56	-0.22	18	1616.19	0.15
8	1608.59	1.75	19	1610.76	0.58
9	1605.69	1.65	20	1622.73	0.61
10	1611.7	-1.36	21	1629.75	0.59
11	1606.67	4.67	22	1620.68	0.66

Then the regression equation model was used to predict the terminal molten steel temperature, and the samples of the model were taken from a steel plant RH refining furnace from November to December 2022 in which 22 sets of 95 furnaces production data were used as test samples. The results are shown in Fig. 6, Fig. 7, Fig. 8 and Table 2. It was found that the regression analysis model predicted a maximum error of 7.93 and the average mean squared error of the prediction was 11.13. The accuracy of the prediction error within ±5°C was 83%, and the accuracy of the error within ±6°C reached 92%. The regression model was not as effective as the neural network in predicting the end-point steel temperature using the regression model because of its weak ability to fit a nonlinear model and the presence of multicollinearity between the model input data.

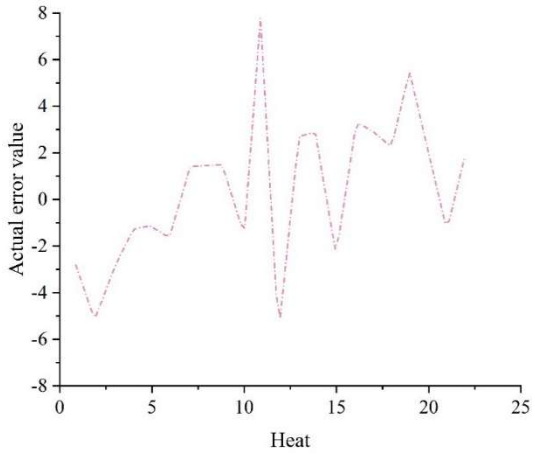

Figure 6: The prediction error of regression model

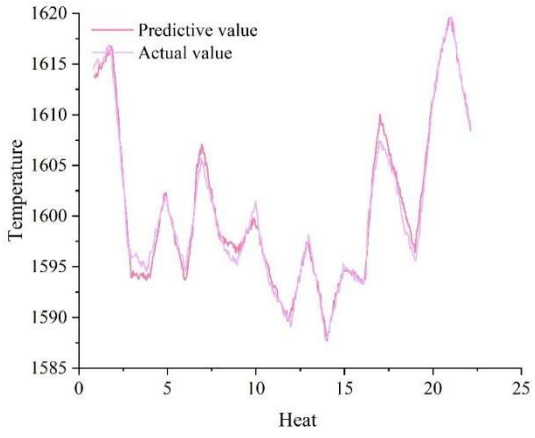

Figure 7: The temperature prediction effect of regression model

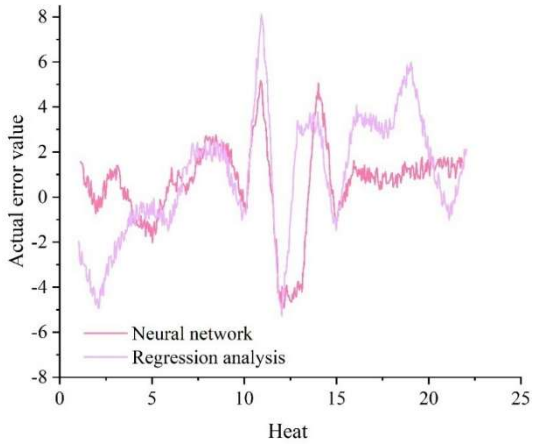

Figure 8: The RMS prediction error comparative of regression model and neural network model

Table 2: The temperature forecast data of regression model

Heat	Forecast temperature (℃)	Error	Heat	Forecast temperature (℃)	Error
1	1624.064	-3.164	12	1599.244	-6.344
2	1626.544	-5.644	13	1607.564	2.336
3	1606.024	-3.124	14	1597.384	2.516
4	1604.484	-1.584	15	1604.804	-2.904
5	1612.284	-1.384	16	1602.984	2.916
6	1604.024	-2.124	17	1617.344	2.556
7	1615.804	1.096	18	1613.104	1.796
8	1607.724	1.176	19	1604.824	5.076
9	1604.804	1.096	20	1620.364	1.536
10	1610.924	-2.024	21	1630.724	-1.824
11	1602.364	7.536	22	1618.244	1.656

III. C. 2) Steel Temperature Prediction for VCD Moments

The samples of VCD moment steel temperature forecasting model are taken from a steel plant RH refining furnace from November to December 2015 in which 95 furnaces production data, of which 70% of the total 61 groups are taken as training samples and the remaining 30% of the total 24 groups are taken as test samples. The parameters of the particle swarm algorithm are chosen as: w_{max} =1.5, w_{min} =0.5, c_{max} =2.6, c_{min} =0.6.The number of units of the neural network implicit layer is chosen as 9, the number of iterations is chosen as 1000, and the target mean squared deviation is chosen as 5, and the results are shown in Fig. 9, Fig. 10, and Fig. 11 as well as Table 3. It was found that the training mean squared error was 29.86, the maximum prediction error was 9.2, and the average mean squared error of prediction was 20.4. 92% accuracy was achieved within ±6°C of the prediction error.

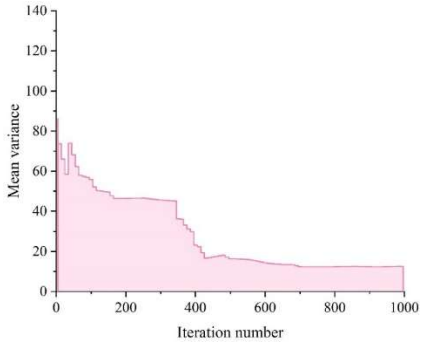

Figure 9: The RMS Training Error of VCD-point model

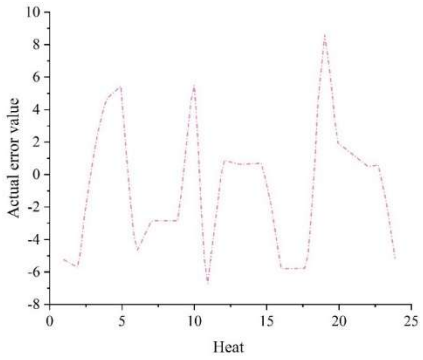

Figure 10: The prediction error of VCD-point model

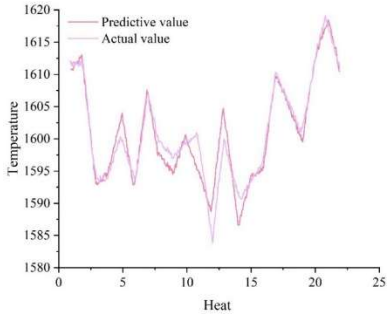

Figure 11: The temperature prediction effect of VCD-point model

Table 3: The temperature forecast data of VCD-point model

Heat	Forecast temperature (℃)	Error	Heat	Forecast temperature (℃)	Error
1	1618.56	-5.46	13	1608.71	0.39
2	1604.14	-6.04	14	1608.71	0.39
3	1622.31	0.79	15	1608.71	0.39
4	1598.74	4.36	16	1624.12	-6.02
5	1598.85	5.25	17	1624.12	-6.02
6	1606.51	-5.41	18	1624.12	-6.02
7	1593.25	-3.15	19	1622.68	8.42
8	1593.25	-3.15	20	1624.41	1.69
9	1593.25	-3.15	21	1626.22	0.88
10	1591.31	5.79	22	1617.82	0.28
11	1607.86	-7.76	23	1617.82	0.28
12	1606.56	0.54	24	1618.56	-5.46

IV. Impact of steel temperature control technology on energy consumption

IV. A. Analysis of the main factors affecting energy consumption

The Pareto rule was used to statistically analyze the energy consumption in the steel production process and to draw a Pareto chart to find out the major and minor influencing factors in the many consumption varieties. In the process of statistics, the liquid steel yield of 97%, straight rolling rate of 89%, and the rate of 98% of the finished product were taken into account. The statistical results are shown in Table 4.

Table 4: Energy consumption sorting for coiled rebar production

Consumable varieties	Code	Corresponding standard coal value (kgce/t)	Proportion %
Electric furnace process-smelting power consumption (kW·h/t)	S1	45.7	39.1%
Steel rolling process-power consumption (kW·h /t)	S2	21.6	18.5%
Electric furnace process-carbon powder (kg/t)	S3	21.5	18.4%

Steel rolling process-Gas furnace (m^3/t)	S4	5.1	4.4%
Electric furnace process-refractory material drying natural gas (m^3/1)	S5	4.4	3.8%
Refinery process-power consumption (kw·h/t)	S6	4.3	3.7%
Electric furnace process-carbon balls (kg/t)	S7	4.1	3.5%
Electric furnace process-natural gas treatment (m^3/t)	S8	2.3	2.0%
Electric furnace process-oxygen (m^3/t)	S9	3.2	2.8%
Electric furnace process-dust removal power consumption (kW·h/t)	S10	1.8	1.5%

Data in accordance with the ton of steel consumption sub-projects produce energy consumption size for sorting, process + classification + consumption sub-projects as the horizontal axis, the use of each consumption sub-projects produce energy consumption as the main vertical axis, the use of each consumption sub-projects produce the use of the cumulative proportion of energy consumption as the secondary vertical axis, in accordance with the principle of the production process of coiled rebar energy consumption of the Pareto as shown in Figure 12.

Coil rebar production process, electric furnace process smelting power, rolling process power, electric furnace smelting carbon powder, rolling heating furnace gas, refining furnace power, electric furnace refractory baking natural gas, electric furnace smelting carbon pellets, electric furnace smelting natural gas, these eight items of energy consumption accounted for more than 90%. Through the Pareto curve, it can be seen that these eight items are the main and secondary factors affecting energy consumption. Among them, electric furnace process smelting electricity, steel rolling process electricity, electric furnace process carbon powder are the main factors affecting energy intensity, accounting for 76%.

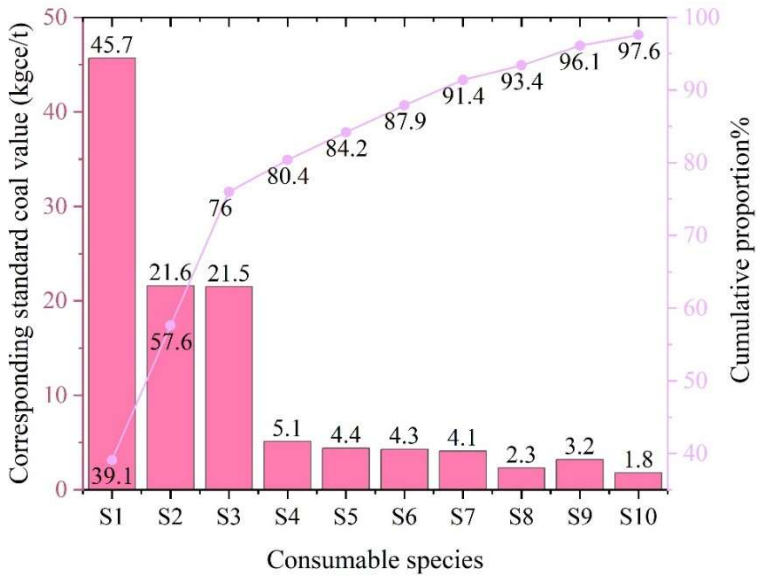

Figure 12: Pareto chart of energy consumption for coiled rebar production

IV. B. Sensitivity analysis of factors affecting energy consumption

IV. B. 1) Calculation of energy consumption within the range of values of the influencing factors

The floating values of each variable are substituted into the energy measurement model to calculate the corresponding energy consumption values under different variables respectively, as shown in Table 5.

Table 5: Energy consumption based on variable parameter

Parameter	The energy consumption value corresponding to the parameter value range				
Electrolytic furnace treatment power consumption (kw·h) (dimensionless range)%	283/(81.4)	311/(92.1)	343/(102)	372/(109.1)	410/(119.6)
Corresponding energy consumption (kgce/t)	108.4	113.2	116.2	119.4	124.1
Electric furnace carbon powder consumption (kg/t) (dimensionless range%)	16/(77)	19/(87)	22/(105)	29/(139)	36/(172)
Corresponding energy consumption (kgce/t)	111.2	113.2	116.3	125.6	130.3

Electricity consumption of rolling steel process (kw·h /t) (dimensionless range%)	142/(88.4)	152/(84.2)	163/(102.5)	171/(109.2)	182/(114.2)
Corresponding energy consumption (kgce/t)	113.4	115	116.5	117.7	118.7
Direct rolling rate%	83	88	92	97	99.7
Corresponding energy consumption (kgce/t)	121.3	118.4	116.5	115.3	110.2
Lumber recovery %	93	95	97	98	99.5
Corresponding energy consumption (kgce/t)	118.5	117.3	116.2	115.1	112
Oxygen treatment by electric furnace (m²/f) (dimensionless range %)	31/(86.2)	33.4/(93.9)	37/(100)	38.3/(109.2)	43/(116.4)
Corresponding energy consumption (kgce/t)	115.4	116.8	116.2	116.5	116.9

The electric furnace smelting power consumption, electric furnace toner consumption, and rolling process power consumption were converted into dimensionless factors to analyze the changes in energy consumption values corresponding to each changing parameter at different magnitudes of change. The influence of each factor on energy consumption is shown in Figure 13.

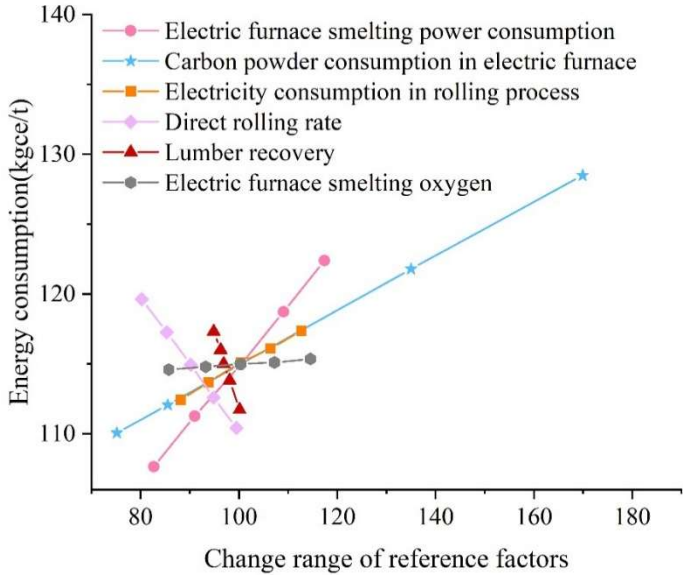

Figure 13: Impact of dimensionless parameters on energy consumption

IV. B. 2) Sensitivity calculations for each parameter

The energy consumption data was processed according to the following equation to obtain the degree of sensitivity under each parameter:

$$S_i = (|(E_i - E_0)|/E_0)/(|(P_i - P_0)|/P_0) \tag{14}$$

$$S_{E\_average} = \sum_{i}^{n}(S_i)/n \tag{15}$$

In Eq. (14) and Eq. (15), S_i represents the sensitivity corresponding to the value of the i variable under a certain parameter, E_i represents the value of the energy consumption corresponding to the i variable under a certain parameter, P_i represents the value of the i variable under a certain parameter, E_0 represents the value of the energy consumption corresponding to the baseline variable under a certain parameter, P_0 represents the baseline variable under a certain parameter, $S_{E\_average}$ represents the average sensitivity coefficient under a certain parameter, and n represents the number of the variables of a certain parameter. The calculation results are shown in Table 6. As can be seen from the table, the sensitivities are, in descending order, as follows: product yield > straight rolling rate > electric furnace smelting power consumption > electric furnace toner consumption > rolling process power consumption > electric furnace smelting oxygen.

Table 6: Sensitivity coefficient corresponding to changing parameters

Parameter	Code	Sensitivity coefficient
lumber recovery %	A1	1.05
Direct rolling rate%	A2	0.41
Electric furnace smelting power consumption (kW h/t)	A3	0.40
Electric furnace carbon powder consumption (kg/t)	A4	0.21
The steel process is electrical consumption (kW h/t).	A5	0.21
Oxygen treatment by electric furnace (m^3/t)	A6	0.04

IV. C. Impact of temperature control technology

IV. C. 1) Impact of temperature forecasting models on electricity consumption

Figure 14 shows the change in electricity consumption per ton of steel before and after the use of the model. In order to compare the change of electricity consumption per ton of steel in the LF furnace refining furnace before and after the use of the model, Figure 14 selects the electricity consumption of each continuous production of 1000 furnaces producing SWRH82B steel before and after the use of the model to be counted and calculated. As can be seen from the figure, the total ton of steel power consumption decreased from 49.5kW-h to 38.7kW-h, the reduction of power consumption per ton of steel is 10.8kW-h, the reduction of power consumption is 21.82%, the price of electricity is calculated at 0.57 yuan/kW-h), the reduction of cost of ton of steel is about 28.2 yuan, and the reduction of production cost is about 28.2 million yuan per year based on the annual production of 1,000,000 tons of steel in the electric furnace.

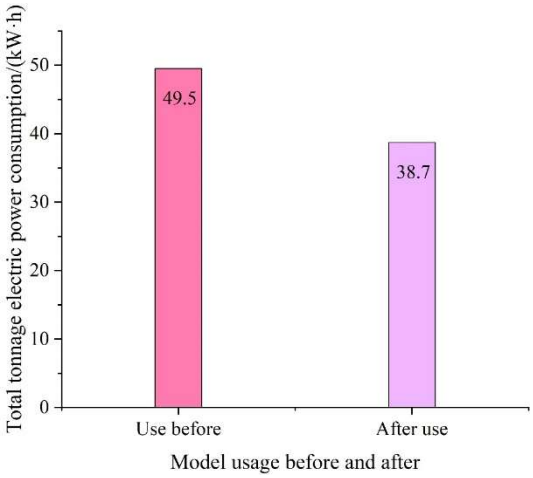

Figure 14: The model uses the change of power consumption per ton of steel before and after

IV. C. 2) **Impact of temperature control technology on refining energy consumption**

In the 12 months' production before the introduction of temperature control technology, the rotary anode refining furnace mainly uses gas and diesel as the main fuel to provide the heat source required for refining, and the combustion fan provides combustion air. After the modification of the rotary anode refining furnace with temperature control technology, the original combustion mode of gas and diesel is canceled, and temperature control technology is used instead, with only diesel as the main fuel, and oxygen with an oxygen-enriched concentration of more than 98% as the combustion air. The energy consumption before and after the application of temperature control technology is shown in Figure 15.

As can be seen from the figure, after the application of temperature control technology, the energy consumption of steel is obviously reduced, and the energy consumption is reduced from more than 100kgce before the application to 44kgce, and this energy consumption index has been relatively stable. With the application of dilute oxygen combustion technology, the energy consumption of tons of anode copper is saved by more than 52%.

Before the application of temperature control technology, each hour can chemical cold crude copper and other copper materials about 7.5t, and after the application of the technology, each hour can chemical cold crude copper and other materials increased to more than 15t. This is due to the temperature control technology furnace without obvious flame, heat diffusion uniformity, strengthen the furnace copper water and furnace temperature of the heat exchange efficiency, significantly improve the cold material materialization speed, improve the material handling capacity, thereby increasing the output per unit of time, combustion of flue gas amount is less, the heat is taken away by the flue gas heat reduction, reducing the energy consumption of steel energy.

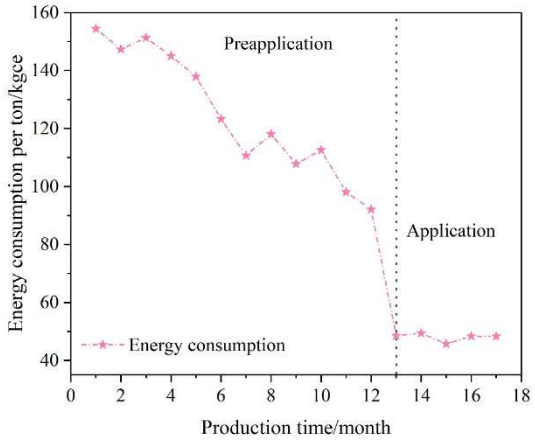

Figure 15: Effect of temperature control technology on refining energy consumption

V. Conclusion

The study uses the improved artificial bee colony algorithm to further optimize the weights and thresholds of the neural network algorithm, and adopts the artificial neural network to establish an intelligent model for steel temperature forecasting. Matlab is used to simulate the model, and the simulation results show that the number of neurons in the hidden layer of the steel temperature forecasting model at the VCD moment is more appropriate to choose 9, and the accuracy of the forecasting error within ±6℃ reaches 92%; the number of neurons in the hidden layer of the steel temperature forecasting model at the terminal moment is more appropriate to choose 16, and the accuracy of the forecasting error within ±5℃ reaches 95%. Applying Pareto's law to determine the major and minor factors affecting energy consumption and carbon emissions, the major factors are smelting power in the electric furnace process, power in the steel rolling process, and carbon powder in the electric furnace process, which account for 76% of the energy consumption of these three items. After applying the temperature control technology, the energy consumption is reduced by more than 50%, the furnace condition is controllable, the operation is simple, the parameters are adjusted quickly, the operation time of a single furnace period is shortened, and the effective operation rate and production capacity per unit time are improved.

References

[1] Jaimes, W., & Maroufi, S. (2020). Sustainability in steelmaking. Current opinion in green and sustainable chemistry, 24, 42-47.
[2] Xing, L., Xiao, W., Zhang, Z., Bao, Y., & Wang, M. (2024). Physical modeling study for process optimization of 300-ton RH vacuum refining furnace. Journal of Sustainable Metallurgy, 10(1), 386-396.
[3] Zhao, L. H., Lin, L., & Wu, Q. F. (2016). Experimental study on sulfur removal from ladle furnace refining slag in hot state by blowing air. International Journal of Minerals, Metallurgy, and Materials, 23, 33-39.
[4] Mullinger, P., & Jenkins, B. (2022). Industrial and process furnaces: principles, design and operation. Butterworth-Heinemann.
[5] Peacey, J. G., & Davenport, W. G. (2016). The iron blast furnace: theory and practice. Elsevier.
[6] Huang, Z., Liu, L., Wang, Z., Wang, C., Liu, Y., Liu, B., ... & Yan, H. (2025). CFD analysis of flow and heat transfer enhancement in a tower-type zinc refining furnace with novel structural designs. Applied Thermal Engineering, 263, 125327.
[7] Pikashov, V. S., & Velikodny, V. A. (2017). Features of the use of refinery gases for heating furnaces and boilers. Energy Technologies & Resource Saving, (2), 3-10.
[8] Kayode, O. I., Adetunji, O. R., Busayo, A., Musibaudeen, I., & Abdulhafiz, A. (2022). Optimization of furnace working index. Borobudur Engineering Review, 2(2), 57-73.
[9] Pyszko, R., Brestovič, T., Jasminská, N., Lázár, M., Machů, M., Puškár, M., & Turisová, R. (2015). Measuring temperature of the atmosphere in the steelmaking furnace. Measurement, 75, 92-103.
[10] Gunasekaran, N., Shanmugaraja, M., Bharathwaaj, R., Dharshini, J. S., Kumar, M. V., & Kumar, P. Y. (2020, December). Analysis and reduction of heat transfer in a furnace of refinery. In Journal of Physics: Conference Series (Vol. 1706, No. 1, p. 012176). IOP Publishing.
[11] Tudon-Martinez, J. C., Lozoya-Santos, J. D. J., Cantu-Perez, A., & Cardenas-Romero, A. (2022). Advanced temperature control applied on an industrial box furnace. Journal of Thermal Science and Engineering Applications, 14(6), 061001.
[12] Zhang, L., Zhao, Y., Liu, S., & Wang, N. (2025). VD furnace discharge temperature control method study. Journal of Control and Decision, 12(3), 489-500.
[13] Vidhyasagar, M., Murali, G., & Balachandran, G. (2021). Thermo-kinetics, mass and heat balance in an energy optimizing furnace for primary steel making. Ironmaking & Steelmaking, 48(1), 97-108.
[14] Cao, S., Hu, X., Xu, W., & Huang, J. (2016). Dual adaptive temperature control of magnesium reduction furnace. International Journal of Modelling, Identification and Control, 26(3), 264-272.
[15] Ahmad, I., Kano, M., Hasebe, S., Kitada, H., & Murata, N. (2014). Gray-box modeling for prediction and control of molten steel temperature in tundish. Journal of Process Control, 24(4), 375-382.
[16] He, Q., Wu, H., Meng, H., Hu, Z., & Xie, Z. (2019). Molten steel level detection by temperature gradients with a neural network. IEEE Access, 7, 69456-69463.

[17] Gunarathne, D. S., Mellin, P., Yang, W., Pettersson, M., & Ljunggren, R. (2016). Performance of an effectively integrated biomass multi-stage gasification system and a steel industry heat treatment furnace. Applied Energy, 170, 353-361.
[18] Na, H., Sun, J., Qiu, Z., Yuan, Y., & Du, T. (2022). Optimization of energy efficiency, energy consumption and CO2 emission in typical iron and steel manufacturing process. Energy, 257, 124822.
[19] Holappa, L. (2020). A general vision for reduction of energy consumption and CO2 emissions from the steel industry. Metals, 10(9), 1117.
[20] Andreev, S. (2019). System of energy-saving optimal control of metal heating process in heat treatment furnaces of rolling mills. Machines, 7(3), 60.
[21] Matino, I., Colla, V., & Baragiola, S. (2017). Electric energy consumption and environmental impact in unconventional EAF steelmaking scenarios. Energy Procedia, 105, 3636-3641.
[22] Mishra, S. B., & Liyakat, K. K. S. (2024). AI-Driven-IoT (AIIoT) Based Decision-Making in Molten Metal Processing. Journal of Industrial Mechanics, 9(2), 45-56.
[23] Liu, Z. Y., Li, C., Fang, X. Y., & Guo, Y. B. (2018). Energy consumption in additive manufacturing of metal parts. Procedia Manufacturing, 26, 834-845.
[24] Xin, Z. C., Zhang, J. S., Zhang, J. G., Zheng, J., Jin, Y., & Liu, Q. (2023). Predicting temperature of molten steel in LF-refining process using IF–ZCA–DNN model. Metallurgical and Materials Transactions B, 54(3), 1181-1194.
[25] Feng, K., He, D., Xu, A., & Wang, H. (2016). End temperature prediction of molten steel in LF based on CBR–BBN. Steel research international, 87(1), 79-86.
[26] WANG, H., WANG, M., LIU, Q., XING, L., & BAO, Y. (2024). Research progress on intelligent control and decision-making models for the ladle furnace refining process. Chinese Journal of Engineering, 46(10), 1739-1752.
[27] Yuan, F., Xu, A. J., & Gu, M. Q. (2021). Development of an improved CBR model for predicting steel temperature in ladle furnace refining. International Journal of Minerals, Metallurgy and Materials, 28, 1321-1331.
[28] Xin, Z. C., Zhang, J. S., Peng, K. X., Zhang, J. G., Zhang, C. H., & Liu, Q. (2024). Modeling of LF refining process: A review. Journal of Iron and Steel Research International, 31(2), 289-317.
[29] He, F., Xu, A., Wang, H., He, D., & Tian, N. (2012). End temperature prediction of molten steel in LF based on CBR. steel research international, 83(11), 1079-1086.
[30] Feng, K., Yang, L., Su, B., Feng, W., & Wang, L. (2022). An integration model for converter molten steel end temperature prediction based on Bayesian formula. steel research international, 93(2), 2100433.
[31] He, D., Song, C., Guo, Y., & Feng, K. (2024). An Error Correction Method Based on CBR for End Temperature Prediction of Molten Steel in Ladle Furnace. ISIJ International, 64(8), 1291-1300.
[32] Qiao, Z., & Wang, B. (2021). Molten steel temperature prediction in ladle furnace using a dynamic ensemble for regression. IEEE Access, 9, 18855-18866.
[33] Wang, X., You, M., Mao, Z., & Yuan, P. (2016). Tree-structure ensemble general regression neural networks applied to predict the molten steel temperature in ladle furnace. Advanced Engineering Informatics, 30(3), 368-375.
[34] Zong-Bao, G. A. O., Hai-Bin, W. U., Jun-Cheng, G. E., Wei, K. O. N. G., & Kai-Di, L. I. U. (2021). Non-Contact Temperature Measurement System of Molten Steel in LF Furnace and Its Application. Journal of Atmospheric and Environmental Optics, 16(1), 74.
[35] Montes-Dorantes, P. N. (2024). Ladle furnace temperature monitoring and control by interval type-2 radial basis function neural network. The International Journal of Advanced Manufacturing Technology, 134(7), 3507-3518.
[36] Yue Chong,Chen Mantong,Lang Yaopu & Liu Qinggang. (2025). Design of high phase-sensitivity BlueP/TMDC heterostructure-based SPR biosensor using improved artificial bee colony algorithm. Nanotechnology and Precision Engineering,8(2),
[37] Yash Pathak,Laxman Prasad Goswami,Bansi Dhar Malhotra & Rishu Chaujar. (2025). Artificial Neural Network based modelling for variational effect on double metal double gate negative capacitance FET. Micro and Nanostructures,206,208225-208225.